CORTEX 128 (2020) 132–142

Available online at www.sciencedirect.com

ScienceDirect

Journal homepage: www.elsevier.com/locate/cortex

Special Issue "Understanding Others": Research Report

Predictive processing account of action perception: Evidence from effective connectivity in the action observation network

Burcu A. Urgen [a,b,c,*] and Ayse P. Saygin [d,e]

[a] Department of Psychology, Bilkent University, Ankara, Turkey
[b] Interdisciplinary Neuroscience Program, Bilkent University, Ankara, Turkey
[c] Aysel Sabuncu Brain Research Center and National Magnetic Resonance Research Center (UMRAM), Ankara, Turkey
[d] Department of Cognitive Science, University of California, San Diego, CA, USA
[e] Neurosciences Graduate Program, University of California, San Diego, CA, USA

ARTICLE INFO

Article history:
Received 28 July 2019
Reviewed 23 September 2019
Revised 19 December 2019
Accepted 17 March 2020
Published online 6 April 2020

Keywords:
Action perception
fMRI
Dynamical causal modeling
Predictive coding

ABSTRACT

Visual perception of actions is supported by a network of brain regions in the occipito-temporal, parietal, and premotor cortex in the primate brain, known as the Action Observation Network (AON). Although there is a growing body of research that characterizes the functional properties of each node of this network, the communication and direction of information flow between the nodes is unclear. According to the predictive coding account of action perception (Kilner, Friston, & Frith, 2007a; 2007b), this network is not a purely feedforward system but has backward connections through which prediction error signals are communicated between the regions of the AON. In the present study, we investigated the effective connectivity of the AON in an experimental setting where the human subjects' predictions about the observed agent were violated, using fMRI and Dynamical Causal Modeling (DCM). We specifically examined the influence of the lowest and highest nodes in the AON hierarchy, pSTS and ventral premotor cortex, respectively, on the middle node, inferior parietal cortex during prediction violation. Our DCM results suggest that the influence on the inferior parietal node is through a feedback connection from ventral premotor cortex during perception of actions that violate people's predictions.

* *Corresponding author*. Department of Psychology, Bilkent University, Ankara, Turkey.
E-mail address: burcu.urgen@bilkent.edu.tr (B.A. Urgen).

https://doi.org/10.1016/j.cortex.2020.03.014
0010-9452/

1. Introduction

Over the last two decades, neurophysiological and neuroimaging studies in primates have identified a network of brain regions in occipito-temporal, parietal and premotor cortex that are associated with visual processing of actions, known as the Action Observation Network (AON, Rizzolatti & Craighero, 2004; Iacoboni & Dapretto, 2006; Saygin, 2007; Caspers, Zilles, Laird, & Eickhoff, 2010; Nelissen et al., 2011; Saygin, 2012). Although significant progress has been made in understanding the neural correlates of action perception, one open question in the field is how the nodes of this network communicate. This question is of particular importance to be able to specify neural mechanisms that go beyond neural correlation.

There has been theoretical work that provide a neuromechanistic account of action perception but empirical work that directly tests it is sparse. One such model by Kilner et al. (2007a; 2007b) proposes that the AON is a predictive system, following the principles of predictive coding (Friston, 2010). In this framework, information is processed throughout the AON by means of forward and backward connections, in contrast to the classic formulation of the AON, which treats action perception strictly as a feedforward process (Giese & Poggio, 2003). More specifically, the middle node of the network, parietal node has reciprocal connections between the occipito-temporal node (the lower node in the hierarchy) and the premotor node (the higher node in the hierarchy) (Fig. 1), which hypothetically enables the forward and backward connections within the system.

There is indeed empirical evidence for the anatomical connectivity of the brain regions that comprise the AON. Our knowledge of the anatomical connectivity patterns in the AON comes primarily from non-human primates. In the macaque monkey, area F5 of the premotor cortex and area PF of the inferior parietal lobule have reciprocal connections (Luppino, Murata, Govoni, & Matelli, 1999). PF also has reciprocal connections with a portion of the posterior superior temporal sulcus (pSTS) that is sensitive to biological movements (Seltzer & Pandya, 1994). Analogous connectivity patterns have been proposed in the human brain (Rushworth, Behrens, & Johansen-Berg, 2006; Igelström & Graziano, 2017).

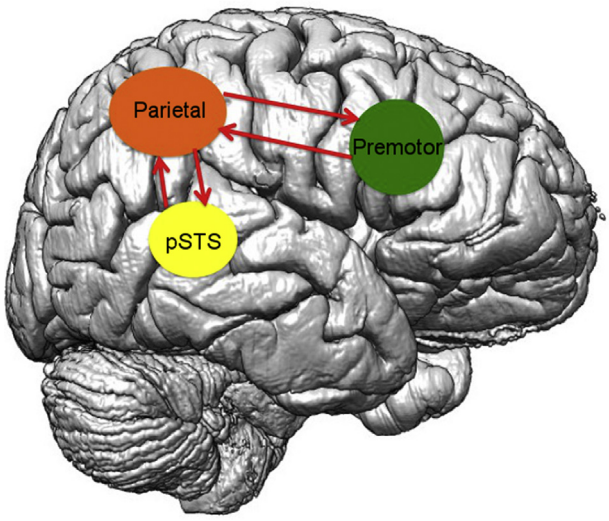

Fig. 1 – Anatomical connectivity between the core nodes of the AON.

There are also a handful of experimental studies that provide support for predictive processing account of action perception. Kilner, Vargas, Duval, Blakemore, and Sirigu (2004), using event-related brain potentials, found that during action observation, the human brain generated a motor-preparation-like negative potential when the action was in a predictable context; no such potential was found when observation occurred within an unpredictable context. In a monkey neurophysiology study, Maranesi, Livi, Fogassi, Rizzolatti, and Bonini (2014) provide direct evidence for predictive activity of visuo-motor neurons in premotor cortex and therefore it is considered to be a foundational step in supporting the predictive processing account of action understanding (Urgen & Miller, 2015). There are also a number of fMRI studies in humans that show that actions are processed by a network that has both forward and backward connections (Cardellicchio, Hilt, Olivier, Fadiga, & D'Ausilio, 2018; Gardner, Goulden, & Cross, 2015; Maffei et al., 2015; Sasaki, Kochiyama, Sugiura, Tanabe, & Sadato, 2012; Sokolov et al., 2018). Among these, Schippers and Keysers (2011) provide evidence for directed information flow from premotor cortex to the other nodes of the action observation network during action prediction. Moreover, a handful of brain stimulation studies show the causal role of motor system, especially premotor cortex in action prediction (Avenanti, Paracampo, Annella, Tidoni, & Aglioti, 2018; Cardellicchio et al., 2018).

In another study, using an fMRI-adaptation paradigm, Saygin, Chaminade, Ishiguro, Driver, and Frith (2012) found that the parietal node of the AON showed more adaptation to actions that violate predictions (via an agent who showed a mismatch between appearance and motion) than to actions that do not (via agent who shows a match between appearance and motion). The authors interpreted the differential adaptation in the parietal cortex for the prediction violations as reflecting prediction error signals generated due to a mismatch between the appearance and movement of the observed actor. Note that the direction of prediction errors is a matter of debate in neuroscience today. While some accounts suggest that prediction errors are transmitted from lower regions to higher regions (Friston, 2010), other accounts propose the opposite (Heeger, 2017).

Regardless of the debate, due to the adaptation-based analysis in Saygin et al. (2012), it could not be determined whether the *influence* on parietal cortex came as a feedforward (bottom-up) influence from earlier visual areas via pSTS, or as a feedback (top-down) modulation from premotor cortex in AON in the mismatch condition. The current study builds on this work and aims to reveal where that influence on parietal cortex might be generated from. Is it a top-down influence from premotor cortex or a bottom-up influence from pSTS? Based on the available evidence (Avenanti et al., 2018; Cardellicchio et al., 2018; Schippers & Keysers, 2011) we hypothesized that the influence on parietal cortex comes from premotor cortex. To test this, we studied the effective connectivity patterns in the AON of the human brain and their modulation by the agent characteristics using functional magnetic resonance imaging (fMRI) and dynamical causal

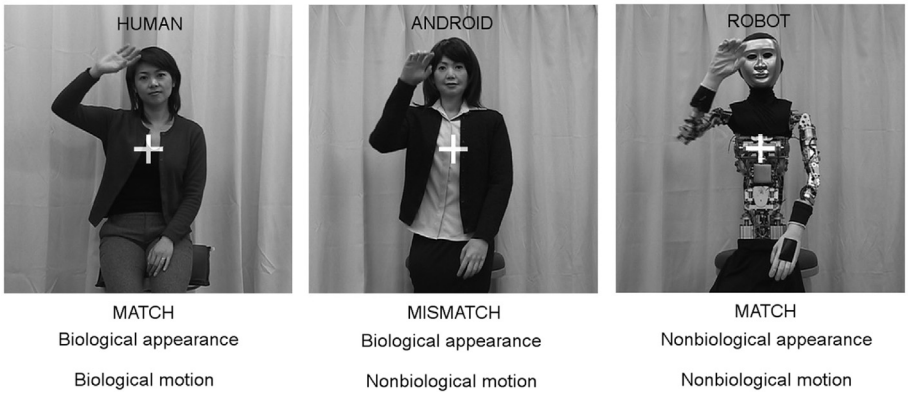

Fig. 2 – Stimuli used in the action perception experiment. There were three agents: Human with biological appearance and biological motion (match between appearance and motion), Android with biological appearance and nonbiological motion (mismatch between appearance and motion), and Robot with nonbiological appearance and nonbiological motion (match between appearance and motion).

modeling (DCM) (Friston, Harrison, & Penny, 2003). Specifically, we investigated the influence of two nodes of the AON, pSTS and premotor cortex over the third node, parietal cortex and how this influence was affected by the mismatch between the appearance and motion of the observed agent.

2. Materials and methods

The fMRI data used in the present study are the same as the one collected in Urgen, Pehlivan, and Saygin (2019). The methodological details are provided below.

2.1. *Participants*

27 subjects (12 females, 15 males) from the student community at the University of California, San Diego participated in the study. Sample size was determined based on previous studies of action observation, in particular the study by Saygin et al. (2012) on which the current study was built on. Data of 4 subjects were not included in the analysis due to excessive head movements (3 subjects) or technical problems during data acquisition (1 subject). The subjects had no history of neurological disorders and normal or corrected-to-normal vision. Informed consent was obtained in accordance with UCSD Human Research Protections Program. The subjects were paid $25 for 1.5 h participation in the study. All ROIs of interest for DCM analysis were identified in 18 subjects so those subjects were included in the DCM analysis.

2.2. *Stimuli*

Stimuli consisted of video clips of actions performed by 3 agents: a human agent, and the humanoid robot Repliee Q2 in two different appearances (human-like and robotic). These agents are referred here as Human, Android, Robot, respectively (Fig. 2, also see Saygin et al., 2012; Urgen, Plank, Ishiguro, Poizner, & Saygin, 2013, 2019) for additional (details about the stimuli).

The agents differed from each other in terms of visual appearance and motion. The Human agent had biological appearance and biological motion, the Android agent had biological appearance and nonbiological motion, and the Robot agent had nonbiological appearance and nonbiological motion. So, in this setting both Human and Robot had a *match* between their appearance and motion (both biological and nonbiological, respectively), whereas Android had a *mismatch* between the appearance and motion. Our earlier study, Urgen, Kutas, & Saygin (2018), indeed has shown that the Android elicited an N400 effect (whereas Human and Robot did not), which is known to be a marker of predictive processing and expectation violation in the case of mismatches. All the agents performed 8 different actions. The actions were comprised of a variety of actions included drinking from a cup, grasping an object, throwing a paper, wiping a table, nudging, turning the body to the right, handwaving, and talking (for introducing herself).

2.3. *Procedure*

Each participant was given exactly the same introduction to the study and the same exposure to the videos as prior knowledge can induce biases against artificial agents (Saygin & Cicekli, 2002). Before starting fMRI scans, subjects were shown each video and were told whether each agent was a human or a robot (and thus were not uncertain about the identity of the agents during the experiment). We recorded fMRI BOLD response as subjects watched 2 s action clips in a total of 8 runs. In each run, the experiment had a block design in which blocks consisted of video clips of one agent type (Human, Android, or Robot, see Fig. 2). The experiment had 18 stimuli blocks (6 Human, 6 Android, 6 Robot) and they were presented in a pseudo-randomized order ensuring that all order combinations were presented (i.e., H-A-R, H-R-A, A-H-R, A-R-H, R-H-A, R-A-H). A rest block followed the presentation of the three blocks of agents. There, subjects fixated on a cross for a time interval varying between 8.1 s and 13.5 s. Each block had 9 trials (8 different actions and

repetition of a randomly chosen action once) with .1 s inter-stimulus interval in between the trials. Each subject was presented a different order of blocks and of stimuli within each block. In order to keep subjects' attention throughout the experiment, an incidental one-back task was performed in which subjects pressed a button whenever a movie was repeated.

2.4. Image acquisition, preprocessing and first-level analysis

We scanned our subjects at the Center for fMRI at UC San Diego using the 3 T GE MR750 scanner (Functional/EPI images: TR = 2.7 s, TE = 30, Flip angle = 90, number of slices = 35, voxel size = 3 mm × 3 mm x 3 mm, 152 volumes in each run, sequential acquisition; Structural images: 172 volumes, 256 × 256 pixel, T1-weighted). The stimuli were presented on a projector through a mirror mounted in the head cover in the scanner. First, the fMRI data of each subject were pre-processed with standard procedures including motion correction, slice-time correction (referenced to 1st slice in the series), normalization, and smoothing (8 mm) using the SPM8 software. Then, two different first-level analyses (i.e., within subject) were performed using a general linear model (GLM). In the first analysis, each agent type (Human, Android, Robot) as well as the rest blocks (fixation) were modeled as a separate condition and beta images were generated for these conditions. This analysis was done to identify the overall activity patterns and determine the nodes or the regions of interest (ROIs) of the AON. After the first level analysis was run for each subject, we ran the second-level random-effects analysis to compute the group level activation map. To this end, we created the contrast [All Agents (Human, Android, Robot) − Fixation] ($p < .001$) and extracted our ROIs from this map (See Section 2.5). The second analysis was done to investigate the modulations in the effective connectivity of the AON via dynamical causal modeling (See Section 2.6). In the second analysis, we defined two conditions: The first condition was defined as *Actions* and consisted of actions of all three agents (Human, Android, Robot) to investigate the modulations of the connections by any action stimulus regardless of agent. The second condition was defined as the *Mismatch* condition, and consisted of the actions only by the Android, which featured a mismatch between appearance and motion, to investigate the modulations of the connections by the Mismatch condition. In this paradigm, we are using "mismatch" in the sense that visual predictions, under a high level representation of biological movement - are violated when watching the human-like robot (i.e., Android) move. In other words, the mismatch is between predictions under a pre-potent generative model of the visual consequences of any given agent (i.e., human-like motion based on human-like appearance) and what is actually observed (non-human like motion). In addition, we also included the *Match* condition to compare with the Mismatch condition, which consisted of the action videos performed by the Human and the Robot, as there was a match between the appearance and motion of these agents. Motion parameters generated in the preprocessing stage were used as regressors in both analyses.

2.5. Identification of ROIs

We identified the ROIs of the AON by contrasting the overall activation patterns for all stimuli conditions compared to fixation ($p < .001$ uncorrected, cluster threshold $k = 5$ voxels) using the first first-level analysis for each subject (described in Section 2.4 above). We chose the central voxel of the activation in each node of the AON and extracted a spherical ROI that contained the subject-specific activation. We did this for all 18 subjects for whom we identified all ROIs of interest. The ROI time series data was then extracted using the principal eigenvariate of all voxels (that survived the threshold of $p < .05$) within a sphere with 4 mm radius.

2.6. Specification of the network models

In order to investigate whether a mismatch between appearance and motion of an agent during action perception was mediated through a bottom-up process from pSTS to inferior parietal cortex, or as a top-down process from ventral premotor cortex to inferior parietal cortex, we analyzed our fMRI data with dynamical causal modeling (DCM).

Dynamical causal modeling (DCM) is an effective connectivity technique to estimate the *directed* connectivity between different regions of interest with fMRI (Friston et al., 2003; Penny, Stephan, Mechelli, & Friston, 2004). DCM consists of two stages: Model specification and estimation, and model selection. In the model specification and estimation stage, several model architectures are specified based on the known anatomy between brain regions of interest and the hypothesis about how the connections might be modulated by the experimental manipulations. Three parameters are estimated: 1) Intrinsic connections between brain regions, 2) How the intrinsic connections are modulated by experimental manipulations, 3) The extrinsic input strength into the system. In the model selection stage, Bayesian Model Selection (BMS) procedure is used to determine the most likely model that generated the observed data. In this procedure, each model architecture in the model space is assigned a probability for explaining the observed data. The model that has the highest probability is then considered to be the "winning" or the optimal model.

To test our hypothesis, we constructed 3 models that consisted of the main three ROIs of the AON, namely pSTS, the inferior parietal node, and the ventral premotor node (See the coordinates listed in Table 2) for each subject and in each hemisphere. To constrain the model space, in each of these models, the intrinsic connections between the ROIs were informed by the known anatomical connections between the regions. As such, pSTS and the parietal node, and the parietal node and the premotor node had reciprocal connections between each other (Fig. 3A). Furthermore, in all models, pSTS was considered to be the node where the visual input entered the system, and all intrinsic connections were modulated by the observation of actions (*Action* condition, see Section 2.4). In this setting, Action condition served both as the visual driving input from pSTS and the modulatory influence on the reciprocal connections of the AON. In other words, the observation of actions was assumed to evoke activity in pSTS first (input to the system), and then subsequently propagated to parietal

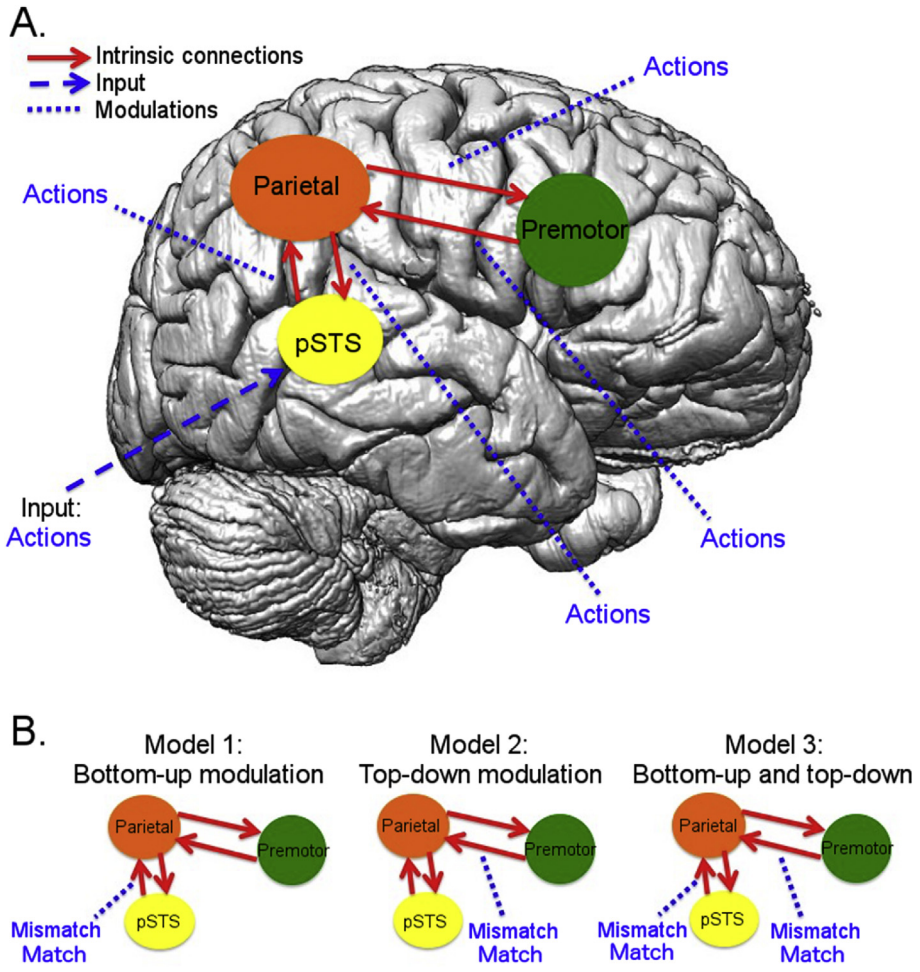

Fig. 3 – DCM models tested in the model space. (A) The DCM model that forms the basis for all tested models in the model space in (B). There are reciprocal intrinsic connections between pSTS and parietal node, and the parietal node and the premotor node informed by anatomy (red arrows). The input to the system is assumed to enter to the AON through pSTS since pSTS gets information from the visual cortex (blue dashed arrow). All the intrinsic connections are modulated by observation of actions (dashed blue lines). (B) The model space that consists of three models that correspond to our hypothesis about how the mismatch condition (as well as the match condition) might modulate the intrinsic connections. Model 1 tests a bottom-up modulation from pSTS to parietal node, Model 2 tests a top-down modulation from premotor node to parietal node, and Models 3 tests both a bottom-up and a top-down modulation.

and premotor cortex based on the known anatomical connections. After the first feedforward flow of information from a lower area to a higher area, feedback from a higher area to a lower area occurred in all models.

The three models differed with regard to which connections were modulated by the *Mismatch* condition (See Section 2.4, Fig. 3B). The first model posits that influence on parietal cortex activity is through connections from pSTS to parietal cortex, i.e., a bottom-up modulation (Model 1). The second model posits that the influence on parietal cortex is through feedback from ventral premotor cortex, i.e., a top-down modulation (Model 2). A third possibility is that the influence would be expressed through both pSTS and premotor cortex connections (Model 3). In all these alternative models, the Match condition was considered to modulate the same connection(s) as of the Mismatch condition to be able to compare the connection strengths in the Match and Mismatch conditions.

In the specification of DCMs, default parameters in SPM8 were used: Modulatory effects were specified to be bilinear, one-state model was run for each region, and stochastic effects were not modeled. Once the parameters were estimated for each model at the individual subject level, random-effects analysis Bayesian Model Selection (BMS) was used to determine the winning model (i.e., the model that best explains the data) at the group level. This method determines a probability for each model, known as the exceedance probability, by pooling the evidence from all subjects. This is the probability that indicates that a model is more likely than any other model tested in the model space. Once the winning model was determined, each of the intrinsic connection strengths and modulatory connection effects were compared with 0 with one-sample *t*-tests ($p < .0001$) to identify the significant connections.

The intrinsic connections indicate the strength of the connectivity between two ROIs. The modulatory connection

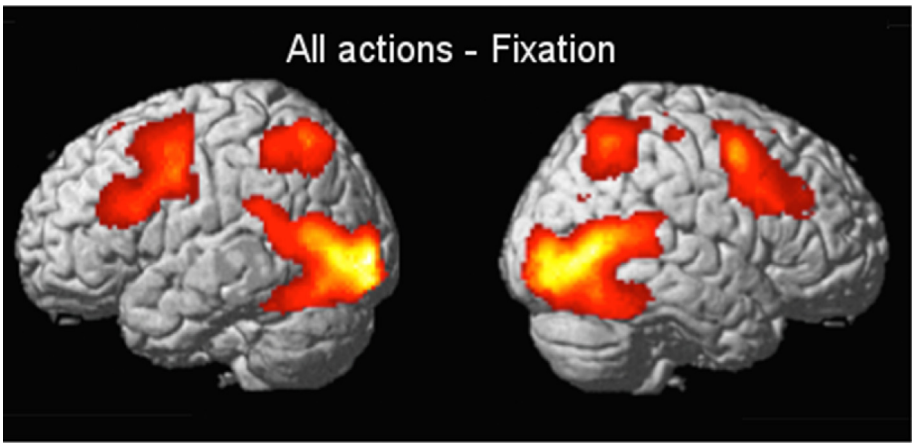

Fig. 4 – Whole brain SPM analysis with the contrast All Agents (Human, Android, Robot) – Fixation ($p < .001$, cluster threshold $k = 5$ voxels) at the group level. The contrast revealed activation in early visual areas extending dorsally to lateral occipital cortex (LOC), and ventrally to inferior temporal cortex, pSTS, parietal cortex, and premotor cortex dorsally and ventrally in both hemispheres. See the coordinates in Table 1.

Table 1 – MNI Coordinates of the peak voxels of the brain regions involved in visual processing of actions based on the All Agents-Fixation contrast in the whole brain GLM analysis (Fig. 3).

MNI coordinates				
x	y	z	Anatomical Name	Brodmann Area
−34	**−92**	**0**	Middle occipital gyrus (left)	BA 17
−26	−92	−10	Inferior occipital gyrus (left)	BA 18
−48	−80	−2	Middle occipital gyrus (left)	BA 19
48	**−74**	**−2**	Inferior temporal gyrus (right)	BA 19
40	−84	−8	Inferior occipital gyrus (right)	BA 19
22	−94	−6	Sub-gyral (right)	BA 18
42	**2**	**56**	Middle frontal gyrus (right)	BA 6
50	34	34	Middle frontal gyrus (right)	BA 9
46	10	30	Inferior frontal gyrus (right)	BA 9
−34	**−58**	**50**	Superior parietal lobule (left)	BA 39
38	**−56**	**52**	Inferior parietal lobule (right)	BA 40
32	−68	28	Sub-gyral (right)	BA 39
−44	**0**	**56**	Middle frontal gyrus (left)	BA 6
−42	−2	38	Middle frontal gyrus (left)	
−60	6	32	Inferior frontal gyrus (left)	BA 6
−6	**12**	**50**	Medial frontal gyrus (left)	BA 6
28	**−6**	**−22**	Amygdala (right)	
−12	**26**	**60**	Superior frontal gyrus (left)	BA 6
8	**−22**	**68**	Medial frontal gyrus (right)	BA 6
38	**−26**	**58**	Precentral gyrus (right)	BA 4

The bold coordinates mean the "Local maxima of the cluster".

strengths on the other hand indicate the change in the effective connectivity value of a connection due to an experimental manipulation. All connections other than the self-connections within an ROI are in Hz. Self-connections (among all intrinsic connections) within an ROI are log scale parameters. This is why it is possible to get negative values, and these values mean weaker connections. The relationship between Hz and log scale is as follows:

C_Hz = C - ((exp (C)/2) + C), where C_Hz is the value in Hz, and C is the log scale parameter.

3. Results

3.1. *Brain regions that are involved in visual processing of actions*

In order to identify the brain regions that were involved in visual processing of actions, we ran the contrast between the observation of actions of all agents (Human, Android, Robot) and the fixation condition. This contrast revealed the

activation in early visual cortex extending dorsally to lateral occipital cortex (LOC) and ventrally to the inferior temporal cortex, as well as the core areas for AON, namely pSTS, parietal regions in the anterior part of the intra-parietal sulcus (AIP) and inferior and superior parts of the parietal lobe, and dorsal and ventral parts of the premotor cortex, all bilaterally ($p < .001$, cluster level 5) (Fig. 4; Table 1 for the coordinates of all activations).

In order to deal with the expansion of model space with increasing number of ROIs and constrain the model space used in the effective connectivity analysis, we extracted ROIs from pSTS, inferior parietal, and ventral premotor cortex in each subject, and excluded the areas in early visual areas. The coordinates of the central voxels of the ROIs averaged over subjects are displayed in Table 2. On average, subjects were 96 percent accurate in the behavioral task.

3.2. *Effective connectivity with DCM and model selection with BMS*

The three DCMs included the three ROIs: pSTS, the inferior parietal node, and the premotor node (ventral premotor cortex). The intrinsic connections included the reciprocal connections between pSTS and the parietal node, and the parietal node and the ventral premotor cortex. The input into the system was considered to enter from pSTS. Observation of all actions was considered to modulate all intrinsic connections (defined by the *Action* condition, see Section 2.4), and the *Mismatch* condition (along with the Match condition) was considered to modulate either the pSTS-parietal connection (Model 1), premotor-parietal connection (Model 2), or both of these connections (Model 3). We chose to model the right and the left hemispheres separately, in the hope of replicating our inferences about the best model architecture – model parameters or effective connectivity changes. In what follows, we report parallel results for the right and left hemisphere.

BMS analysis on the three DCMs showed that Model 2 was the winning (optimal) model in both hemispheres, whose probability was .50 in the left and .55 in the right (Fig. 5). The next best model on the left was Model 1 whose probability was .27, and followed by the least likely model, Model 3, whose probability was .23. On the right hemisphere, the winning model, Model 2, was followed by Model 3, whose probability was, .23 and the least likely model, Model 1's probability was .21.

The intrinsic connection strengths between the ROIs in the winning model, Model 2, are listed in Table 3. All connection strengths were found to be significant (greater than 0 by a one-sample t-test, $p < .0001$) confirming the anatomical connectivity of each pair of regions. In addition, the connection directed from pSTS to the parietal node was estimated to be stronger than the other three connections (parietal to pSTS, parietal to premotor, premotor to parietal) both in the left and the right hemisphere. Note that self-connections within an ROI (e.g., pSTS to pSTS) are log scale parameters whereas the other parameters are in Hz. This is why it is possible to get negative values in the case of self-connections (e.g., pSTS to pSTS connection is –.4960 in Table 3). Negative values mean weak connections and positive values mean strong connections.

Table 2 – The MNI coordinates of central voxels of the ROIs used in the DCM analysis averaged across subjects. pSTS: posterior superior temporal sulcus, STG: superior temporal gyrus, MTG: middle temporal gyrus, IPL: inferior parietal lobule, IFG: inferior frontal gyrus. Values in parenthesis under x, y, z coordinates indicate the standard error of the mean.

	Average MNI coordinates of the central voxels of ROIs in DCM analysis			
	Left hemisphere		Right hemisphere	
Node names in DCM	x y z (Standard error of mean)	Anatomical name/Brodmann Area	x y z (Standard error of mean)	Anatomical name/Brodmann Area
pSTS	−50 -53 7 (1 2 1)	STG/BA 39	53 -44 8 (1 2 1)	MTG/BA 22
Parietal cortex	−37 -42 44 (1 1 1)	IPL/BA 7	37 -42 47 (1 1 1)	Subgyral/BA 7
Premotor cortex	−44 6 29 (1 1 1)	IFG/BA 6	47 9 28 (1 2 1)	IFG/BA 44

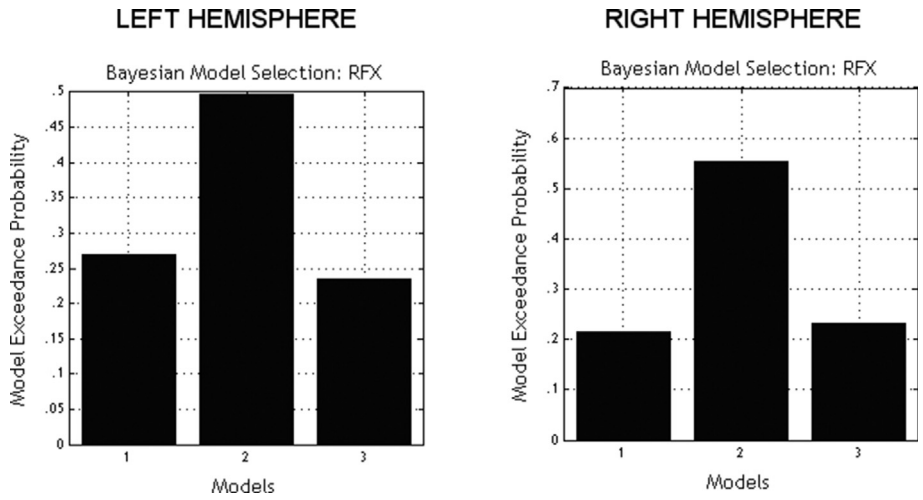

Fig. 5 – The exceedance probability of each model in the model space. Image on the left shows the results of the model testing in the left hemisphere, and the one on the right shows the results of the right hemisphere. In both hemispheres, Model 2 has the highest probability.

Table 3 – The parameters of the intrinsic connectivity that begins with the endogenous activity of actions in the winning model (Model 2) in both hemispheres. The values in the table indicate the mean connection strength across all subjects.

		FROM					
TO		Left hemisphere			Right hemisphere		
		pSTS	Parietal	Premotor	pSTS	Parietal	Premotor
	pSTS	−.4960	.0414	–	−.4964	.0342	–
	Parietal	.1976	−.4993	.0070	.2168	−.4994	.0071
	Premotor	–	.0483	−.5000	–	.0461	−.5000

Table 4 – The parameters of the modulatory activity of actions in the winning model (Model 2) in both hemispheres. The values in the table indicate the mean connection strength across all subjects.

		FROM					
TO		Left hemisphere			Right hemisphere		
		pSTS	Parietal	Premotor	pSTS	Parietal	Premotor
	pSTS	–	.0105	–	–	.0077	–
	Parietal	.0796	–	.0005	.0850	–	.0005
	Premotor	–	.0132	–	–	.0121	–

On the other hand, in the winning model Model 2, the modulatory effects of *Actions* on all four connections were found to be significant (greater than 0 as inferred by post-hoc (confirmatory) classical one sample *t*-tests, $p < .0001$). The strength of the modulatory effects of *Actions* is shown in Table 4 and displayed on the right hemisphere in Fig. 6 together with input strength. The connection between pSTS and the parietal node was modulated most strongly. The modulatory effect of the Mismatch condition on the premotor-parietal connection was .00026 on the left hemisphere, and .00032 on the right. This means that the change in the effective connectivity value of the premotor-parietal connection due to the experimental manipulation (i.e., mismatch) is .00026 on the left, and .00032 on the right. Although this seems to be a small change, it was a statistically significant change ($p < .0001$). On the other hand, the modulatory effect of the Match condition on the same connection (premotor-to-parietal) was less than that of the Mismatch condition: it was .00024 on the left hemisphere, and .00019 on the right, but the differences were not significant (Left: $t(17) = .13$, $P = .89$; Right: $t(17) = .64$, $P = .53$). The input strength was −.0059 on the left hemisphere, and −.0057 on the right hemisphere.

4. Discussion

The brain regions that are involved in visual processing of actions are relatively well established in cognitive neuroscience (Caspers et al., 2010; Saygin, 2012). However, how the information flows between these regions is less understood. In the present study, we aimed to estimate the effective connectivity patterns between the core nodes of the Action

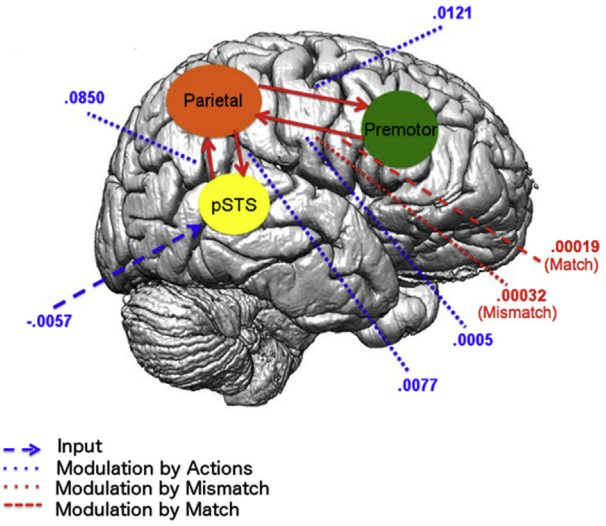

Fig. 6 – Modulatory connection strengths in the winning model, Model 2 across subjects (only right hemisphere is shown for display purposes). The mean values for action modulations for both hemispheres are also listed in Table 4. Modulations by actions are shown by the blue dotted lines. Modulation by the mismatch condition is shown by the red dotted line, and the match condition is shown with the red dashed line. All connection strengths were significantly different from 0 (as inferred by post-hoc (confirmatory) classical one-sample *t*-tests, $P < .0001$).

Observation Network and how these connections were modulated by prediction violations during action perception. Our study was primarily motivated by the findings of Saygin et al. (2012), who reported that the parietal node of the AON showed differential activity during observation of actions which were performed by an agent who possessed a mismatch between appearance and motion (a biological appearance but mechanical motion) compared to other agents who possessed a match between appearance and motion (biological appearance and motion or mechanical appearance and motion). Within the predictive coding account of action perception (Kilner et al., 2007a; 2007b), one question that has been of interest to us was whether that differential activity in parietal cortex was a top-down effect from premotor cortex or a bottom-up effect from pSTS. The current study addressed this question using fMRI and DCM.

We constructed three models to test our hypothesis. First of all, informed by well-known anatomy in the primate brain, in all these models, we created reciprocal intrinsic connections between pSTS and the inferior parietal node, and the inferior parietal node and the ventral premotor node. The input into the system was considered to enter from pSTS, which was a reasonable assumption given the involvement of pSTS in visual analysis of form and motion information in observed actions (Urgen et al., 2019; Vangeneugden et al., 2011, 2009). In addition, in all these models, we assumed that observation of actions modulated all intrinsic connections. We then constructed three specific models that corresponded to our hypotheses: A first model in which the connection from pSTS to parietal cortex was modulated, a second model in which the connection from the premotor cortex to the parietal cortex was modulated, and a third model in which both connections were modulated by the mismatch condition (the agent that exhibited a mismatch between appearance and motion). Our results show that the most likely model that best explains the data is a model in which the connection from the premotor cortex to the parietal cortex was modulated, which indicates a top-down influence.

Confirmatory classical tests of the parameter estimates of the optimal model confirmed that all the intrinsic connections were greater than zero, reflecting the well-known anatomy between these regions (Luppino, et al., 1999; Seltzer & Pandya, 1994; Rushworth et al., 2006). The strongest intrinsic connectivity was between the pSTS and the inferior parietal node. On the other hand, all of the intrinsic connections were modulated significantly by the observation of actions, which is consistent with an earlier DCM study of action observation (Sasaki et al., 2012). These results suggest that action-related information is processed via both forward and backward connections in the AON. On the other hand, the mismatch between appearance and motion of an observed agent during action perception was likely mediated primarily via a backward connection from the premotor to the parietal node of the AON.

These results provide support for the predictive processing account of action perception (Kilner et al., 2007a; 2007b), which proposes that there are reciprocal connections between the three levels of the AON, and prediction error signals depend upon top-down predictions. Our data shows that actions are not only processed by a network that has forward and backward connections consistent with previous work (Cardellicchio et al., 2018; Gardner et al., 2015; Maffei et al., 2015; Sasaki et al., 2012; Sokolov et al., 2018) but also provides evidence that in the case of prediction violations (e.g., when a moving agent exhibits a mismatch between appearance and motion), the premotor node of the AON has an influence on the inferior parietal node – the lower node in the hierarchy. The nature of this signal is a matter of debate: in the context of the most well known predictive coding theory (Friston, 2010), it may be a *prediction* signal whereas in an alternative predictive processing theory of cortical function (Heeger, 2017), it may be a *prediction error* signal. Nevertheless, these results are consistent with previous studies that show the *causal* role of premotor cortex in action observation (Avenanti et al., 2018; Schippers & Keysers, 2011).

In our interpretation above, we noted that an increase in the backward connectivity from the premotor node to the parietal node could be interpreted in terms of an increased sensitivity to descending afferents. This speaks to an alternative way of modeling attentional set in paradigms such as ours; namely, by trying to explain differential responses in terms of the excitability or self-connectivity of each region. In other words, we could have explored a larger model space in which both between and within-region connections were allowed to change during the mismatch conditions. Although we will pursue this in future work, this would not allow us to disambiguate between our primary hypotheses; namely, whether the activations in the parietal node can be attributed to backward or forward connections.

We note again that the sort of mismatch induced by our paradigm rests upon the assumption that there is some prepotent set of predictions about the visual consequences of movement that are violated when watching a robot move. We base this upon the simple fact that humans are, a priori, predisposed to generating predictions about the movement of conspecifics – and similar looking agents such as humanoid robots, as evidenced by our previous work (Urgen et al., 2018).

The comparison of the modulatory effect of the Mismatch condition on the premotor-parietal connection in the winning model, with that of the Match condition showed no significant differences at the group level (although the Mismatch condition resulted in a numerically greater modulation than the Match condition). However, this does not necessarily disqualify our conclusion that the influence on the inferior parietal node is through feedback connections from ventral premotor during perception of actions that violate people's predictions. There could still be directed connectivity from premotor cortex to parietal cortex when there is no prediction violation. Indeed, this is why we included the Action condition as a modulatory effect in all of the reciprocal connections, and we found that all the connections were modulated significantly by this condition. So, we would like to emphasize that our primary question was not whether the match and mismatch conditions differentially modulated the connection strengths but rather which connection was modulated significantly in the case of prediction violations. The finding that the match and mismatch conditions did not differ significantly does not necessarily conflict with this result.

Finally, some caveats must be noted. BMS is a Bayesian approach, which assigns a probability to each model tested in the model space and constrained by the experimental design. Future studies should test the generality of this model during action observation under different task demands. For instance, the mismatch between the two visual cues, appearance and motion is a particular case where predictions are violated during action perception. Novel prediction paradigms in which there are mismatches between different visual cues, multi-sensory cues, or even cognitive cues (e.g., as in Costantini et al., 2005; Koelewijn, van Schie, Bekkering, Oostenveld, & Jensen, 2008; Stapel, Hunnius, van Elk, & Bekkering, 2010) should be tested in future studies of action observation with effective connectivity techniques.

5. Preregistration

No part of the study procedures was pre-registered prior to the research being conducted. No part of the study analyses was pre-registered prior to the research being conducted.

6. Sample size

We report how we determined our sample size, all data exclusions, all inclusion/exclusion criteria, whether inclusion/exclusion criteria were established prior to data analysis, all manipulations, and all measures in the study (page 6–7).

Open practices

The study in this article earned an Open Data badge for transparent practices. Materials and data for the study are available at https://osf.io/kmgpw/?view_only=7d860e6536f4431fa4e75e27fe776904.

The stimuli used in this study belong to the Saygin-Ishiguro action database and the authors do not have the legal authority to share these videos publicly. Legal authority is held by Ayse P. Saygin (UC San Diego) and Hiroshi Ishiguro (Osaka University) and the materials can be obtained by contacting them through email: asaygin@cogsci.ucsd.edu or ishiguro@sys.es.osaka-u.ac.jp.

CRediT authorship contribution statement

Burcu A. Urgen: Conceptualization, Methodology, Software, Investigation, Writing - original draft, Writing - review & editing, Visualization. **Ayse P. Saygin:** Conceptualization, Investigation, Writing - original draft, Writing - review & editing, Visualization, Supervision, Project administration, Funding acquisition.

Acknowledgments

This study was supported by Qualcomm Institute, Kavli Institute for Brain and Mind, NSF and DARPA. The authors also would like to thank Edward Nguyen for his help in fMRI data collection.

REFERENCES

Avenanti, A., Paracampo, R., Annella, L., Tidoni, E., & Aglioti, S. M. (2018). Boosting and decreasing action prediction abilities through excitatory and inhibitory tDCS of inferior frontal cortex. *Cerebral Cortex, 28*(4), 1282–1296.

Cardellicchio, P., Hilt, P. M., Olivier, E., Fadiga, L., & D'Ausilio, A. (2018). Early modulation of intra-cortical inhibition during the observation of action mistakes. *Scientific Reports, 8*, 1784.

Caspers, S., Zilles, K., Laird, A. R., & Eickhoff, S. B. (2010). ALE meta-analysis of action observation and imitation in the human brain. *Neuroimage, 50*(3), 1148–1167.

Costantini, M., Galati, G., Ferretti, A., Caulo, M., Tartaro, A., Romani, G. L., et al. (2005). Neural systems underlying observation of humanly impossible movements: An FMRI study. *Cerebral Cortex, 15*, 1761–1767.

Friston, K. J. (2010). The free-energy principle: A unified brain theory? *Nature Reviews Neuroscience, 11*, 127–138.

Friston, K. J., Harrison, L., & Penny, W. (2003). Dynamical causal modeling. *Neuroimage, 19*(4), 1273–1302.

Gardner, T., Goulden, N., & Cross, E. S. (2015). Dynamic modulation of the action observation network by movement familiarity. *Journal of Neuroscience, 35*(4), 1561–1572.

Giese, M., & Poggio, T. (2003). Neural mechanisms for the recognition of biological movements. *Nature Reviews, 4*, 179–192.

Heeger, D. (2017). Theory of cortical function. *Proceedings of the National Academy of Sciences of the United States of America, 114*(8), 1773–1782.

Iacoboni, M., & Dapretto, M. (2006). The mirror neuron system and the consequences of its dysfunction. *Nature Reviews Neuroscience, 7*(12), 942–951.

Igelström, K. M., & Graziano, M. S. (2017). The inferior parietal lobule and temporoparietal junction: A network perspective. *Neuropsychologia, S0028-3932*(17), 30001–30005.

Kilner, J. M., Friston, K. J., & Frith, C. D. (2007a). The mirror-neuron system: A Bayesian perspective. *Neuroreport, 18*, 619–623.

Kilner, J. M., Friston, K. J., & Frith, C. D. (2007b). Predictive coding: An account of the mirror neuron system. *Cognitive Processing, 8*, 159–166.

Kilner, J. M., Vargas, C., Duval, S., Blakemore, S. J., & Sirigu, A. (2004). Motor activation prior to observation of a predicted movement. *Nature Neuroscience, 7*, 1299–1301.

Koelewijn, T., van Schie, H. T., Bekkering, H., Oostenveld, R., & Jensen, O. (2008). Motor-cortical beta oscillations are modulated by correctness of observed action. *Neuroimage, 40*, 767–775.

Luppino, G., Murata, A., Govoni, P., & Matelli, M. (1999). Largely segregated parietofrontal connections linking rostral intraparietal cortex (areas AIP and VIP) and the ventral premotor cortex (areas F5 and F4). *Experimental Brain Research, 128*(1–2), 181–187.

Maffei, V., Indovina, I., Macaluso, E., Ivanenko, Y. P., Orban, G. A., & Lacquaniti, F. (2015). Visual gravity cues in the interpretation of biological movements: Neural correlates in humans. *Neuroimage, 104*, 221–230.

Maranesi, M., Livi, A., Fogassi, L., Rizzolatti, G., & Bonini, L. (2014). Mirror neuron activation prior to action observation in a predictable context. *Journal of Neuroscience, 34*, 14827–14832.

Nelissen, K., Borra, E., Gerbella, M., Rozzi, S., Luppino, G., Vandu_el, W., et al. (2011). Action observation circuits in the macaque monkey cortex. *Journal of Neuroscience, 31*, 3743–3756.

Penny, W. D., Stephan, K. E., Mechelli, A., & Friston, K. J. (2004). Comparing dynamical causal models. *Neuroimage, 22*(3), 1157–1172.

Rizzolatti, G., & Craighero, L. (2004). The mirror-neuron system. *Annual Reviews of Neuroscience, 27*, 169–192.

Rushworth, M. F. S., Behrens, T. E. J., & Johansen-Berg, H. (2006). Connection patterns distinguish 3 regions of human parietal cortex. *Cerebral Cortex, 16*(10), 1418–1430.

Sasaki, A. T., Kochiyama, T., Sugiura, M., Tanabe, H. C., & Sadato, N. (2012). Neural networks for action representation: A functional magnetic-resonance imaging and dynamic causal modeling study. *Frontiers in Human Neuroscience, 6*, 236.

Saygin, A. P. (2007). Superior temporal and premotor brain areas necessary for biological motion perception. *Brain: a Journal of Neurology, 130*(9), 2452–2461.

Saygin, A. P. (2012). Biological motion perception and the brain: Neuropsychological and neuroimaging studies. In K. Johnson, & M. Shiffrar (Eds.), People watching: Social, perceptual, and neurophysiological Studies of body perception. *Oxford series in visual cognition*. Oxford University Press.

Saygin, A. P., Chaminade, T., Ishiguro, H., Driver, J., & Frith, C. (2012). The thing that should not be: Predictive coding and the uncanny valley in perceiving human and humanoid robot actions. *[Social Cognitive and Affective Neuroscience Electronic Resource], 7*(4), 413–422.

Saygin, A. P., & Cicekli, I. (2002). Pragmatics in human-computer conversations. *Journal of Pragmatics, 34*, 227–258. https://doi.org/10.1016/S0378-2166(02)80001-7.

Schippers, M. B., & Keysers, C. (2011). Mapping the flow of information within the putative mirror neuron system during gesture observation. *Neuroimage, 57*(1), 37–44.

Seltzer, B., & Pandya, D. N. (1994). Parietal, temporal, and occipital projections to cortex of the superior temporal sulcus in the rhesus monkey: A retrograde tracer study. *The Journal of Comparative Neurology, 343*(3).

Sokolov, A., Zeidman, P., Erb, M., Ryvlin, P., Friston, K. J., & Pavlova, M. A. (2018). Structural and effective brain connectivity underlying biological motion detection. *Proceedings of the National Academy of Sciences of the United States of America, 115*(51), E12034–E12042.

Stapel, J. C., Hunnius, S., van Elk, M., & Bekkering, H. (2010). Motor activation during observation of unusual versus ordinary actions in infancy. *Social Neuroscience, 5*, 451–460.

Urgen, B. A., Kutas, M., & Saygin, A. P. (2018). Uncanny valley as a window into predictive processing in the social brain. *Neuropsychologia, 114*, 181–185.

Urgen, B. A., & Miller, L. E. (2015). Towards an empirically grounded predictive coding account of action understanding. *Journal of Neuroscience, 35*(12), 4789–4791.

Urgen, B. A., Pehlivan, S., & Saygin, A. P. (2019). Distinct representations in occipito-temporal, parietal, and premotor cortex during action perception revealed by fMRI and computational modeling. *Neuropsychologia, 127*, 35–47.

Urgen, B. A., Plank, M., Ishiguro, H., Poizner, H., & Saygin, A. P. (2013). EEG Theta and Mu oscillations during perception of human and robot actions. *Frontiers in Neurorobotics, 7*, 19. https://doi.org/10.3389/fnbot.2013.00019.

Vangeneugden, J., De Mazière, P. A., Van Hulle, M. M., Jaeggli, T., Van Gool, L., & Vogels, R. (2011). Distinct mechanisms for coding of visual actions in macaque temporal cortex. Journal of Neuroscience, *31*(2), 385–401.

Vangeneugden, J., Pollick, F., & Vogels, R. (2009). Functional differentiation of macaque visual temporal cortical neurons using a parametric action space. *Cerebral Cortex, 19*(3), 593–611.